Use of the Angular Correlation Function
to Identify Background SNO Events
SNO-STR-2000-032

William Heintzelman
University of Pennsylvania

January 15, 2001

Angular Correlation Function for a Continuous Distribution

Suppose we have a distribution of photons from an event, with $\sigma(\Omega)$ the photon density per unit solid angle in the direction Ω, also given by angles (θ, ϕ). Let η' be the angle between two elements of solid angle. Define

$$C(\eta) = f \int_{\Omega'} \int_{\Omega} \frac{\sigma(\Omega')\ \sigma(\Omega)}{\sin \eta'}\ \delta(\eta' - \eta)\ d\Omega\ d\Omega' \tag{1}$$

where f is a normalizing factor such that $C(\eta) = 1$ for all η $(0 \leq \eta \leq \pi)$ when $\sigma(\Omega)$ is uniform. $C(\eta)$ is the integral of $\frac{\sigma(\Omega')\sigma(\Omega)}{\sin \eta}$ over all pairs of elements of solid angle such that the angle between the two elements is η. When multiplied by f, it becomes the ratio of the number of photon pairs at a separation η for the given distribution divided by the number at that separation for an isotropic distribution. If the distribution $\sigma(\Omega)$ has a concentration of photons at a single spot, we will have $C(\eta) > 1$ for small η and $C(\eta) < 1$ elsewhere. For concentrations at two anti-parallel directions, we will have $C(\eta) > 1$ for $0 \leq \eta \leq \Delta$ and $\pi - \Delta \leq \eta \leq \pi$, where Δ is small. In general, $C(\eta)$ will vary with the distribution, and we might be able to use $C(\eta)$ to distinguish between distributions of photons from different types of SNO events.

Suppose $\sigma(\Omega) = N/4\pi$, *i.e.,* there are N photons distributed isotropically. Then

$$C(\eta) = f\ (\frac{N}{4\pi})^2 \int_{\Omega'} \int_{\Omega} \frac{\delta(\eta' - \eta)}{\sin \eta'}\ d\Omega\ d\Omega' \tag{2}$$

For a given element of solid angle $d\Omega'$, in choosing the coordinate system for integrating over Ω, select (θ, ϕ) such that $\theta = \eta'$. Then

$$C(\eta) = f\ (\frac{N}{4\pi})^2 \int_{\Omega'} \int_0^{2\pi} \int_0^{\pi} \frac{\delta(\theta - \eta)}{\sin \theta}\ \sin \theta\ d\theta\ d\phi\ d\Omega' = f\ (\frac{N}{4\pi})^2 \int_{\Omega'} \int_0^{2\pi} d\phi\ d\Omega' = f\ \frac{N^2}{2} \tag{3}$$

Because we want $C(\eta) = 1$ for an isotropic distribution, we set $f = 2/N^2$.

Angular Correlation Function for a Discrete Distribution

If we replace the integral definition of $C(\eta)$ with a sum over discrete elements of solid angle, we have for a given increment $\Delta\eta$ in η,

$$C(\eta)\Delta\eta = f \sum_{\Delta\Omega} \sum_{\Delta\Omega'} \frac{\sigma(\Omega')\ \sigma(\Omega)\ \Delta\Omega'\ \Delta\Omega}{\sin\eta} \tag{4}$$

where the sums are over elements of solid angle such that $|\eta - \eta'| \leq \Delta\eta/2$.

For an observed event,

$$C(\eta) = \frac{2fN_{pr}(\eta)}{\Delta\eta \sin\eta} \tag{5}$$

where $N_{pr}(\eta)$ is the observed number of photon pairs separated by angles in the interval $(\eta - \Delta\eta/2, \eta + \Delta\eta/2)$, and a factor of 2 is inserted under the assumption that each pair is counted only once. Using the value f=2/N(N-1) (adjusting for the fact that in the discrete case, N photons form N(N-1)/2 unique pairs),

$$C(\eta) = \frac{4}{N(N-1)} \frac{N_{pr}(\eta)}{\Delta\eta\ \sin\eta} \tag{6}$$

Alternatively, we can write C as a function of $w = cos(\eta)$, obtaining

$$C(w) = \frac{4}{N(N-1)} \frac{N_{pr}(w)}{\Delta w} \tag{7}$$

or

$$C(w) = \frac{4}{N(N-1)\Delta w} \sum_{i=1}^{N} \sum_{j=i+1}^{N} \delta(w, w_{ij}) \tag{8}$$

where w_{ij} is the cosine of the angle between the i^{th} and j^{th} photons and $\delta(w, w_{ij}) = 1$ for $|w - w_{ij}| \leq \Delta w/2$ and $\delta(w, w_{ij}) = 0$ otherwise.

Now consider the case where there are N_{ev} Čerenkov light-producing events, all identical in the sense that the light is produced by a charged track of the same type and energy. If we weight the events equally, our estimate of $C(w)$ based on the complete sample is

$$C(w) = \frac{1}{N_{ev}} \sum_{i=1}^{N_{ev}} C_i(w) \tag{9}$$

where $C_i(w)$ is the event correlation function for the i^{th} event.

Application to SNO

Detection of a photon by a PMT in the SNO detector provides us with a measurement of one point on the photon track, with some uncertainty due to the finite size of the PMT/concentrator assembly. But to calculate the angular correlation function, we need a second point. The electrons that radiate Čerenkov photons have short tracks relative to the size of the detector, so we can consider the photons to have come from a single point; and in the results shown in this paper, I have taken that point to be the event location as estimated by the grid fitter, although the output from any of the other fitters could be used. Uncertainty in the estimated event location introduces additional uncertainty in knowledge of the photon tracks.

Correlation Functions for Various Cases

The characteristics of the angular correlation function were studied for various abstract distributions, Monte Carlo events, and events from SNO.

Figures 1 and 2 are correlation functions calculated by summing over discrete elements of solid angle for two simple distributions (Equation 4). Figure 1 is for a "45° cap", which has a uniform density over angles within 45° of a fixed vector and a density of zero elsewhere. This correlation function is of course zero for cosines less than zero, since there are no non-zero-density elements of solid angle separated by more than 90°. Figure 2 is for a "35°–45° band", which has a uniform density in a circular band separated from a fixed vector on one edge by 35° and on the other edge by 45°, and zero density elsewhere. Again the function is zero for $\eta > 90°$. In addition, we see a peak at a cosine of about 0.22, corresponding to approximately 77°, as one would expect because of the pairing of solid angle elements on opposite sides of the circular band. Note that there is a difference in the scales of the two figures as well as in their shapes, which is important because the absolute value of the functions has significance.

Figure 3 is from Monte Carlo simulations of electrons of various energies, with tracks starting at the center of the SNO detector heading downward initially (in the –z direction). The solid curve is for a kinetic energy of 5 MeV; the dashed curve is 1.5 MeV; and the dotted curve is 20 MeV. Only photon tracks that originated near the center of the detector were included, to minimize the effects of scattering and reflections. The pair angles were calculated using the center of the detector as the vertex, and the points where the simulated photons crossed the sphere of radius 600 cm (*i.e.,* just inside the AV) as the other ends of the photon tracks. The numbers of events simulated were 4000, 2000, and 1000 for the 1.5 MeV, 5 MeV, and 20 MeV cases, respectively. In the 1.5 MeV case, 44 of the generated events were not included in the correlation function computation because the number of photons was less that 15. All curves show a characteristic "knee" at a value corresponding to about 80°which is approximately twice the Čerenkov angle, with the knee moving to larger angles at higher energies. (The Čerenkov angle is 41.3° for 5 MeV electrons.) It is notable how similar the three functions are, in spite of the wide range of energies and large difference in the numbers of photons produced per event. (The average number of photons per event was 32, 155, and 669 for 1.5 MeV, 5 MeV, and 20 MeV, respectively.)

Figure 4 is from Monte Carlo simulations of 5 MeV electrons. Three curves are shown. The solid curve is the correlation function calculated using the points where simulated photons crossed the sphere of radius 600 cm in the outward direction, as in the preceding figure. The dashed curve was calculated using the points at which outward traveling photons (regardless of their most recent interaction vertex) crossed the sphere of radius 825 cm (just inside the PSUP). Relative to the first curve, this curve is shifted towards the value 1. That is, it is more like a uniform distribution, presumably because now we are including more photons that have scattered or reflected, rather than arriving undisturbed from their origins. Note also the upturn at a cosine of -1, which may be due to near-perpendicular reflections of photons to the opposite side of the detector.

The dotted curve was calculated using hit PMT locations from a separate simulation

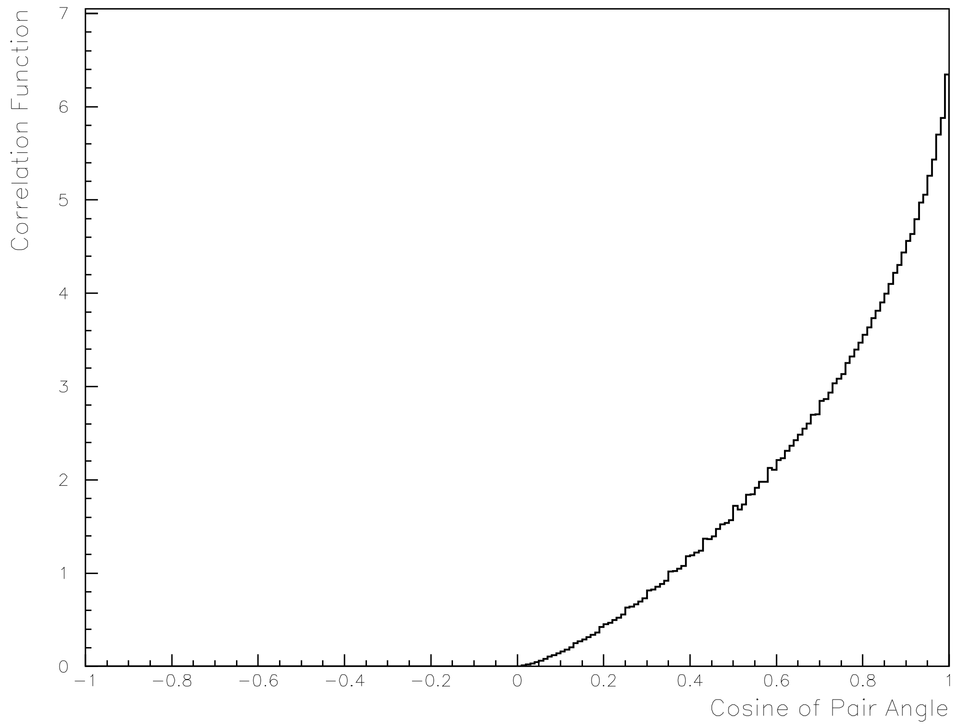

Figure 1: Correlation Function, 45° Cap

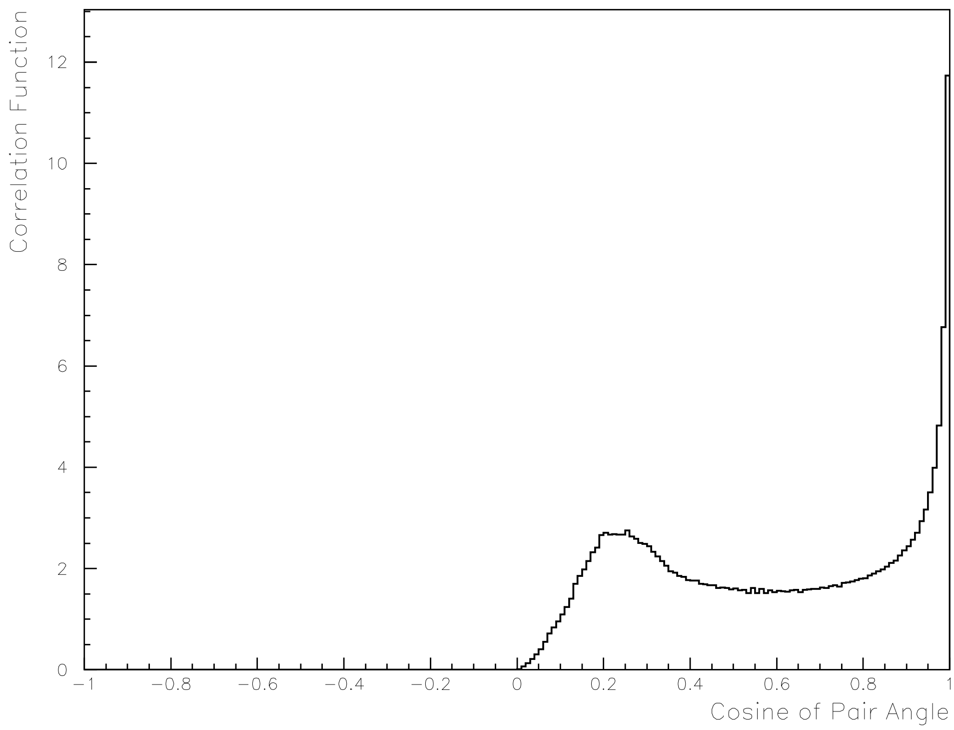

Figure 2: Correlation Function, 35°–45° Band

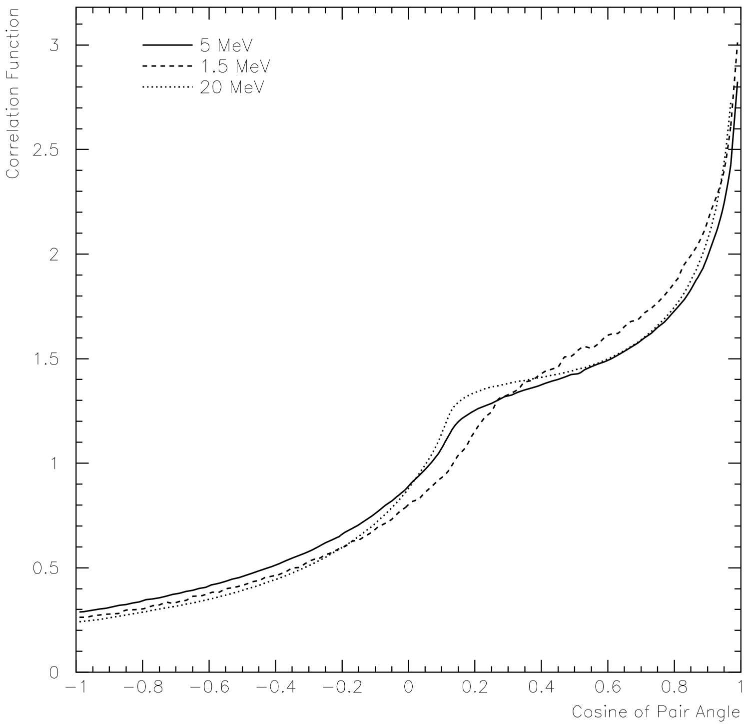

Figure 3: Correlation Functions, Electrons at 1.5, 5, and 20 MeV

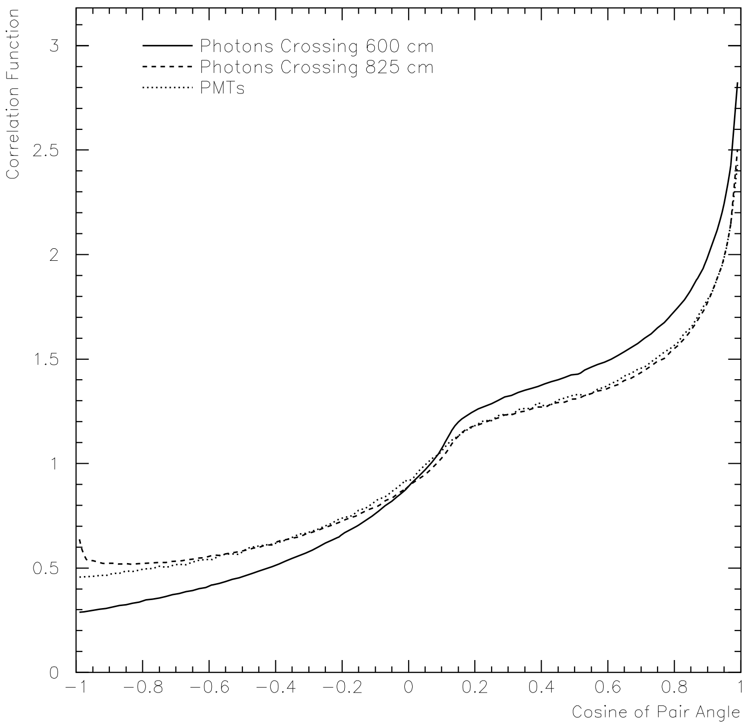

Figure 4: Correlation Functions from Photons and PMTs, 5 MeV Electrons

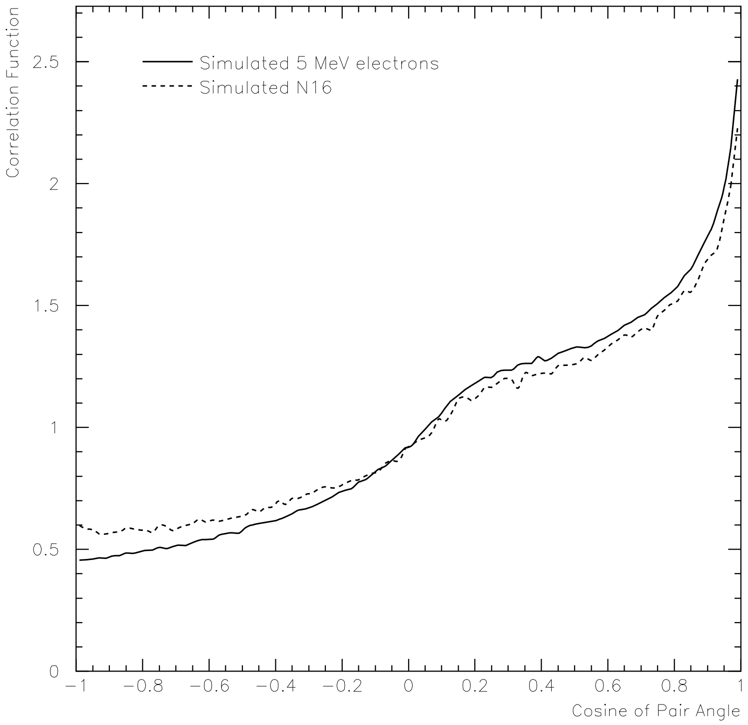

Figure 5: Correlation Functions for Simulated Electrons and Simulated ^{16}N

of isotropic 5 MeV electrons whose starting points were distributed uniformly in the AV. As discussed earlier, the event locations determined by the Grid Fitter were used as the vertices for angle calculations. No PMT noise was included in the simulation. The curve is very close to the dashed curve, indicating that when averaged over numerous events the function is not affected significantly by the use of PMT positions rather than photon tracks or by the event location if the proper vertex is used in the calculation, even if it is not known exactly.

A number of Monte Carlo simulations were done to observe the effect of various changes. In the runs done to this point, the PMTs were assumed to be noiseless. A 5 MeV electron run was made with an assumed average noise rate of 500 Hz. The correlation function obtained was virtually identical with the case of no PMT noise. Perhaps this is not surprising, because at an average rate of 500 Hz, if we take the maximum interval over which PMT hits are collected for an event to be 390 ns, the expected number of noise hits in an event is only 1.9.

The solid line in Figure 5 is same correlation function calculated from PMT hits for simulated 5 MeV electrons that was shown in the preceding figure. The dashed line is for simulated events from the ^{16}N source with locations distributed uniformly in the AV. The curve for the ^{16}N is slightly flatter than that for 5 MeV electrons, probably because of the higher probability that the photons in a gamma-initiated event will be produced by more than one charged track, and hence will be more dispersed in direction.

Figure 6 shows correlation functions for real events recorded with the ^{16}N source

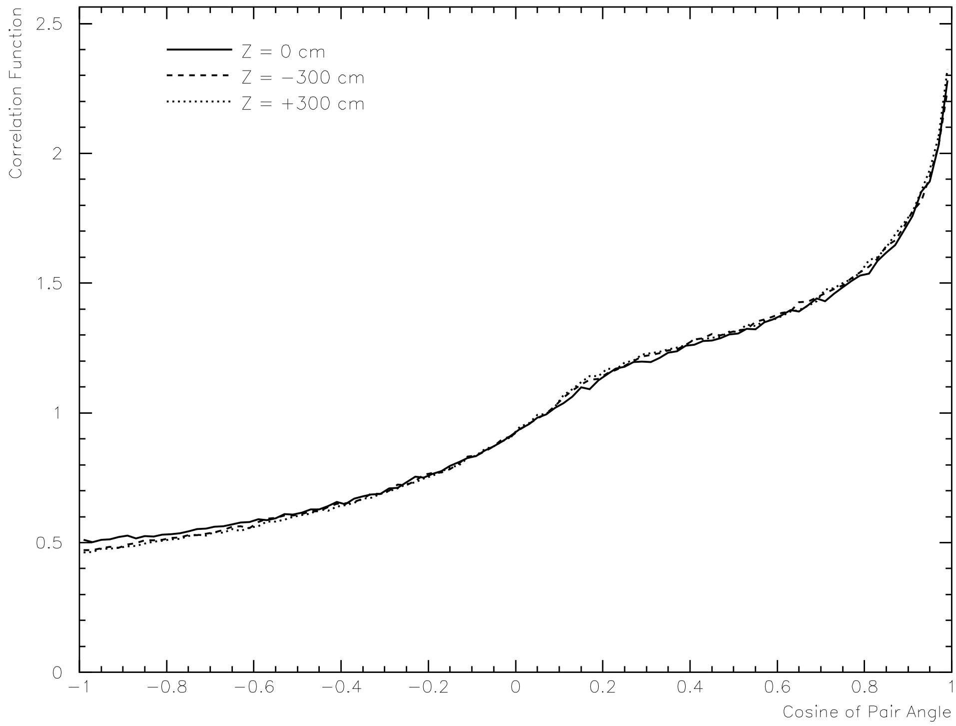

Figure 6: Correlation Functions, ^{16}N at z = 0, –300, & +300 cm

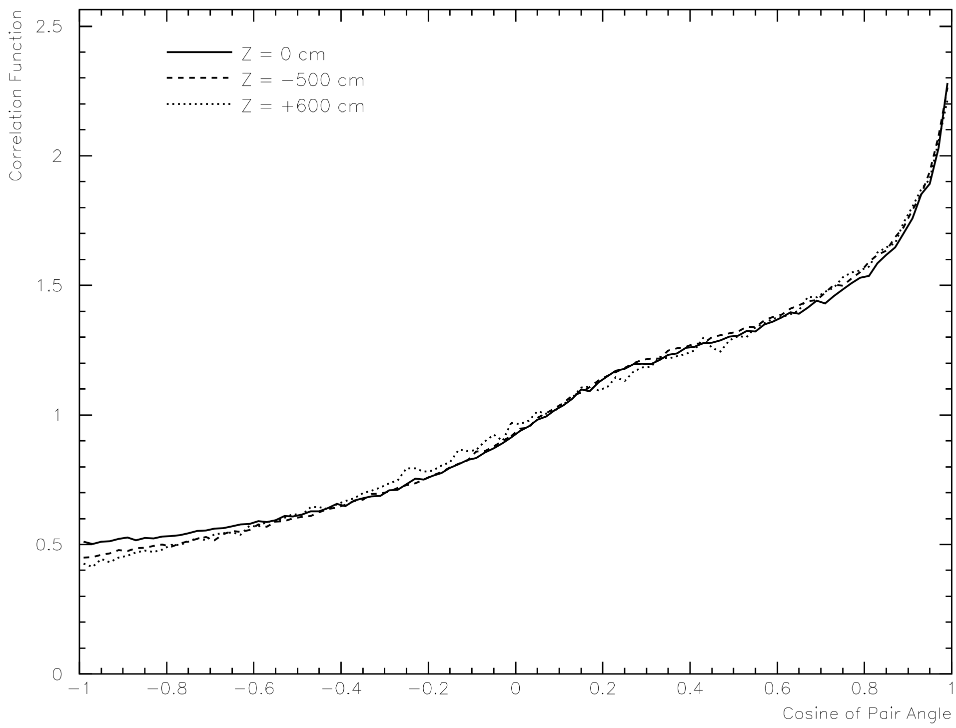

Figure 7: Correlation Functions, ^{16}N at z = 0, –500, & +600 cm

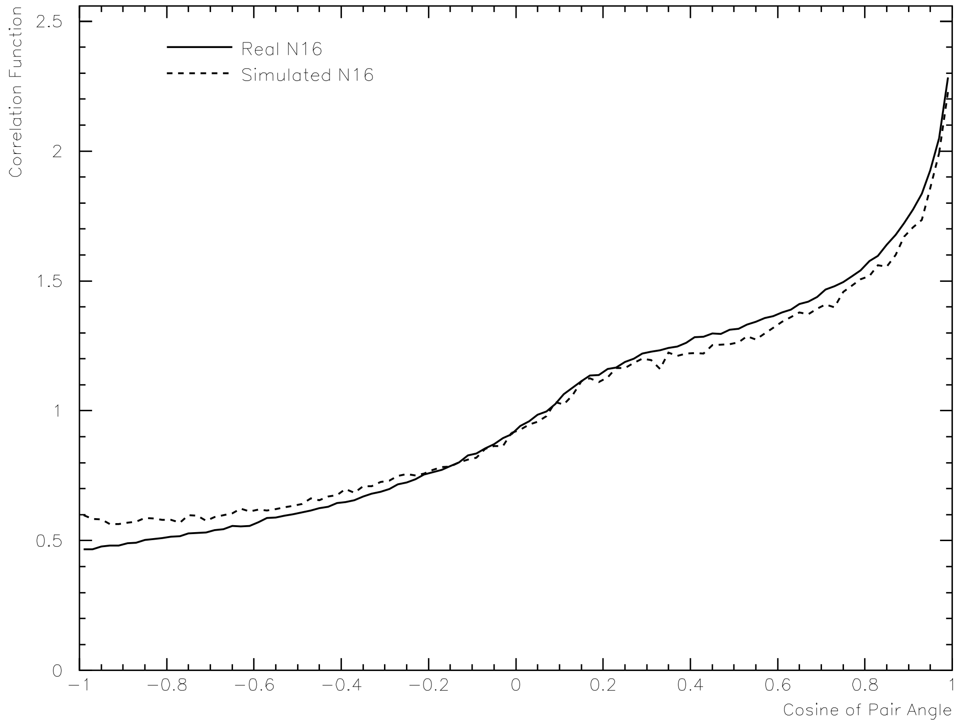

Figure 8: Correlation Functions, Real & Simulated ^{16}N

in the detector (collected after being triggered by the source). There are three curves, for source locations at z = –300 cm, 0 cm, and +300 cm; the x and y coordinates were zero. The curves have the same characteristic shape as in the Monte Carlo simulation of 5 MeV electrons, and there is little difference among the curves. Figure 7 shows the curves for z = –500 cm, 0 cm, and +600 cm. The results are similar.

Figure 8 has two curves: one is the correlation function for a combined sample of real ^{16}N events at z = –300 and z = +300 cm, and the other is for simulated ^{16}N events uniformly distributed in the AV. The function for the real events is steeper, indicating perhaps that there is less scattering and reflection in the detector than modeled by SNOMAN.

In general, one expects scattering and reflection to make the distribution of hit PMTs more uniform and to mask differences between types of events. Therefore, a "time exclusion window" (TEW) cut was applied to the hit PMTs. As noted before, in most events the Čerenkov photons are all produced within a relatively short distance of each other. For point events, the greatest difference in photon arrival time at the PMTs is approximately $2r/v$, where r is the distance of the event from the center of the detector and v is the speed of light in water. Therefore a variable time window cut was applied with the width of the window given in nanoseconds by $2r/v + 10$, where the speed of light in water was taken to be 21.75 cm/ns, and 10 ns is a pad to allow for reconstruction error. The largest set of hit PMTs was found whose hit times were all within the time window of each other, and the calculation of the correlation function was done with this smaller set of PMTs.

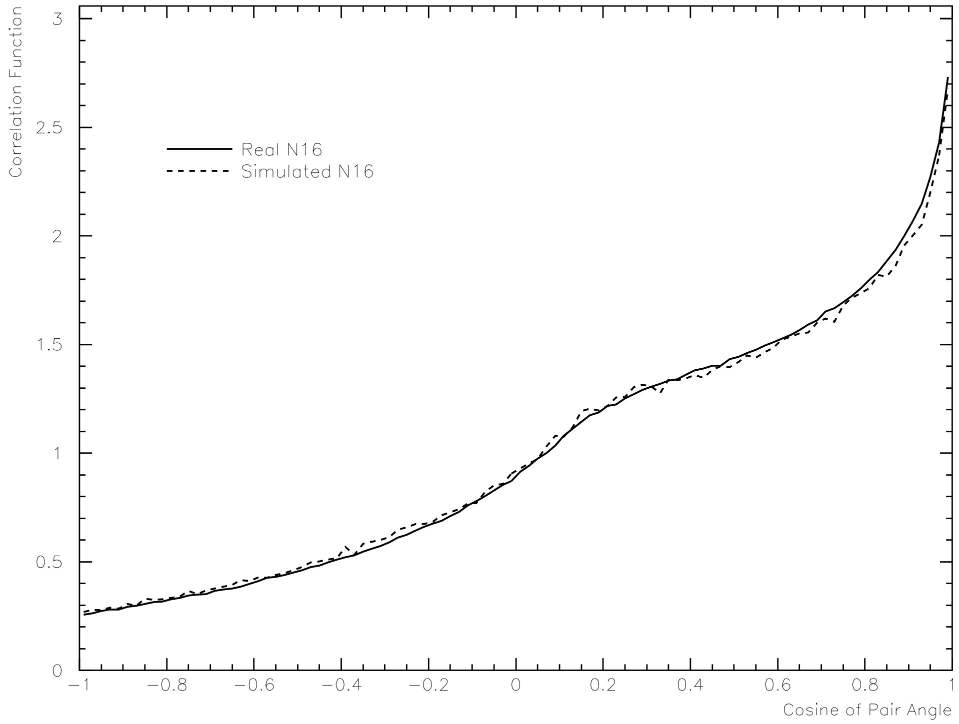

Figure 9: Correlation Functions, Real & Simulated ^{16}N , with TEW

Figure 9 shows the curves for the same two cases as in Figure 8, except that the time exclusion window cut has been applied. Now the curves for the real and simulated ^{16}N events nearly coincide.

Figure 10 has curves with the time exclusion window for three different types of suspected background events: a subset of the "Golden Flasher" events, ring-of-fire events, and neck events. All of these correlation functions lack the characteristic shape that we have seen in both simulated and real events in which Čerenkov light is produced. Note also that there is a large difference in the scale: for these types of events the peak at small angles is much larger than for Čerenkov events, and the value at large angles is correspondingly smaller.

The Correlation Chi-Square

The differences observed in the angular correlation function between Čerenkov -light events on the one hand and the various types of suspected background events on the other hand, lead one to think that it may be possible to use the correlation function to identify background. One would like to have a statistic that quantifies the deviation of the correlation function for an individual event from that of a standard Čerenkov event. It was decided that before calculating such statistics, the normalization of the function should be changed so it integrates to one. The value in each bin is then the fraction of pairs with separation angles falling in the bin. In addition, the number of bins used in the calculations was chosen to be 40, so that on average there would not

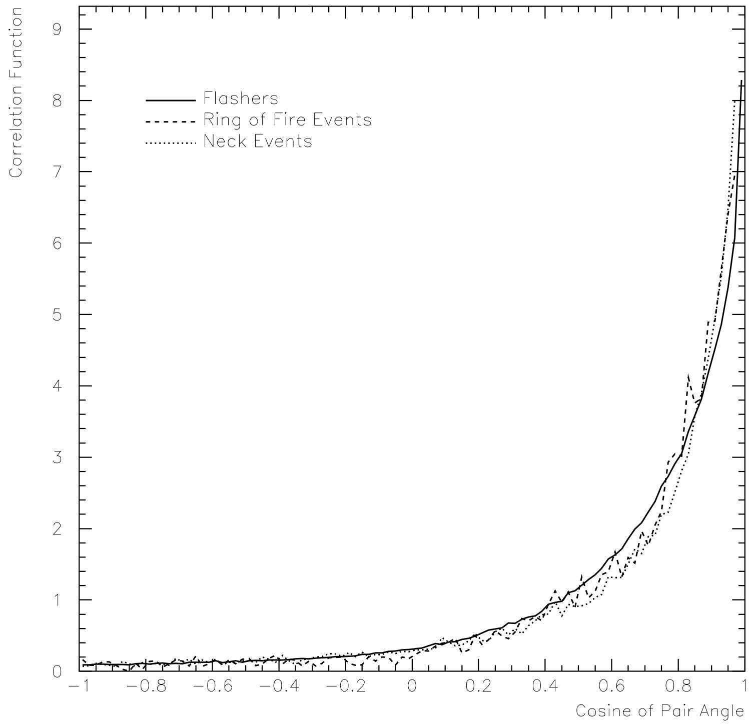

Figure 10: Correlation Functions, Suspected Background, with TEW

be too few pairs in each bin for N_{hit} as low as 20.

Because the correlation function for Čerenkov events changes little over a wide range of energies, it was thought initially that a single standard function might suffice for comparisons at all values of N_{hit}. Following the form of a standard chi-square, one could calculate a statistic like

$$\sum_i \frac{(C_i - C_{S,i})^2}{\sigma_i^2} \tag{10}$$

where C_i is the value of $C(\eta)$ calculated in the i^{th} bin for the event under consideration, $C_{S,i}$ is the value of the standard correlation function in the i^{th} bin, and σ_i is the uncertainty in C_i. Although this statistic has the form of a chi-square and can reasonably be expected to be a measure of the deviation of the event correlation function from the standard function, because the values of $C(\eta)$ in the various bins are not statistically independent, we cannot expect it to have a chi-square distribution. Consider what happens when an additional photon is added to an event that already has N photons. By the addition of one photon, N new pairs are formed, affecting the value of $C(\eta)$ in as many as N different bins. Therefore the values in the various bins must be statistically dependent. In addition, it may be that the degree of correlation between the bin values is a function of N_{hit}. Both of these hypotheses were confirmed.

A large number of electron-initiated events were simulated with total electron energies uniformly distributed between 3 MeV and 9 MeV. Average angular correlation functions were calculated for events with the same N_{hit}, along with covariance matrices for the bin values of the correlation functions. Correlation coefficients were calculated

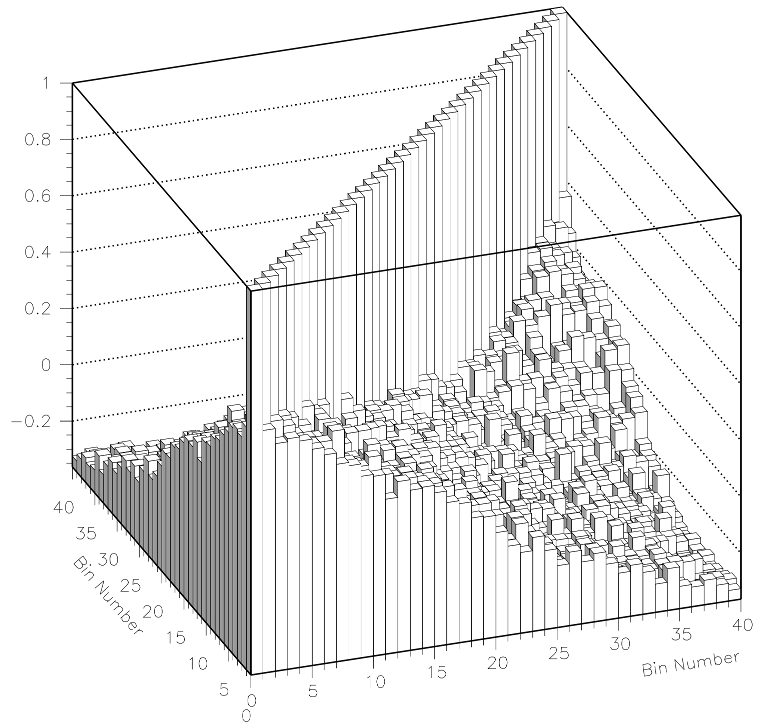

Figure 11: Inter-Bin Correlation Coefficients, with TEW, $N_{hit} = 20$

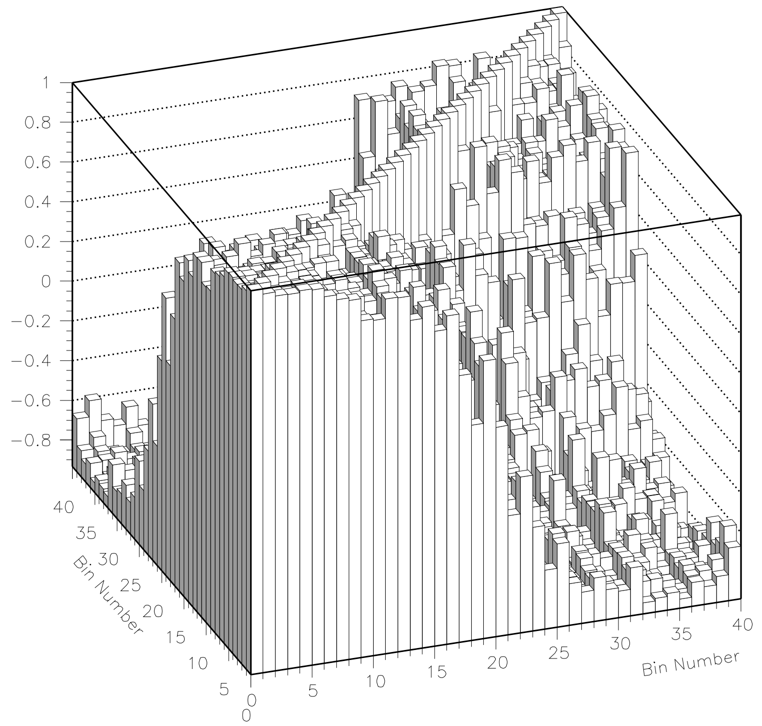

Figure 12: Inter-Bin Correlation Coefficients, with TEW, $N_{hit} = 60$

from the covariances. Figures 11 and 12 are plots of the matrices of correlation coefficients for N_{hit} equal to 20 and 60, respectively. We see that there are significant non-zero values aside from those on the diagonal. Bin values tend to be positively correlated with those in nearby bins, especially at large and small angles (small and large bin numbers respectively) and the values for large angles tend to be negatively correlated with the values for small angles. Furthermore, the correlation coefficients are a strong function of N_{hit}.

For correlated random variables from a multivariate normal distribution, the statistic

$$(X - \mu)^T V^{-1} (X - \mu) \tag{11}$$

does have a chi-square distribution. Here X is the vector of values of the random variables, μ is the vector of their means, and V is the covariance matrix. Although the bin values of the angular correlation function surely do not have a multivariate normal distribution, for sufficiently large N_{hit} we should be able to treat them as if they do. Note, however, that there is a relationship among the bin occupancies, namely that their sum is one. Consequently, the chi-square that we compute has only 39 degrees of freedom, and we must consider only 39 of the 40 bin values in computing it. If we attempt a calculation including all 40 bins, we will obtain a covariance matrix that is not positive definite, having one eigenvalue equal to zero.

The simulated electron events were divided into samples for single values of N_{hit}, and correlation functions and covariance matrices were calculated for each sample up to an N_{hit} value of 70, with and without the time exclusion window. Using the resulting functions as standard functions, the events were reprocessed and chi-square values were calculated for each event using the expression above and applying the appropriate standard function and covariance matrix for each event. Figure 13 shows the results. The histograms have approximately the shape expected of a chi-square distribution with 39 degrees of freedom. For each event the probability was calculated that with a true chi-square distribution with 39 degrees of freedom, one would observe a value greater than the value observed in the event. The distribution of that quantity is shown in Figure 14. If the two distributions in Figure 13 were really chi-square, then the plots in Figure 14 should be horizontal lines within statistical variations. The shapes of these plots indicate that both without and with the TEW, there are excesses of events with large and small values of the correlation chi-square, relative to a true chi-square distribution. However, this does not invalidate use of the correlation chi-square to separate types of events.

Separation of Fake Blind Flashers

Josh Klein created a file of more than 40,000 "fake blind flashers" by removing hits on the flasher PMT and other PMTs in the same card from the event data for real suspected flasher events. Correlation chi-squares were calculated for the fake blind flashers (FBFs) that reconstructed inside the AV, totaling 8689. Because the FBFs have much larger N_{hit} values (up to 350 for events that reconstruct inside the AV), additional events initiated by electrons with total energies between 9 MeV and 20 MeV were simulated to extend the N_{hit} range covered by standard functions up to

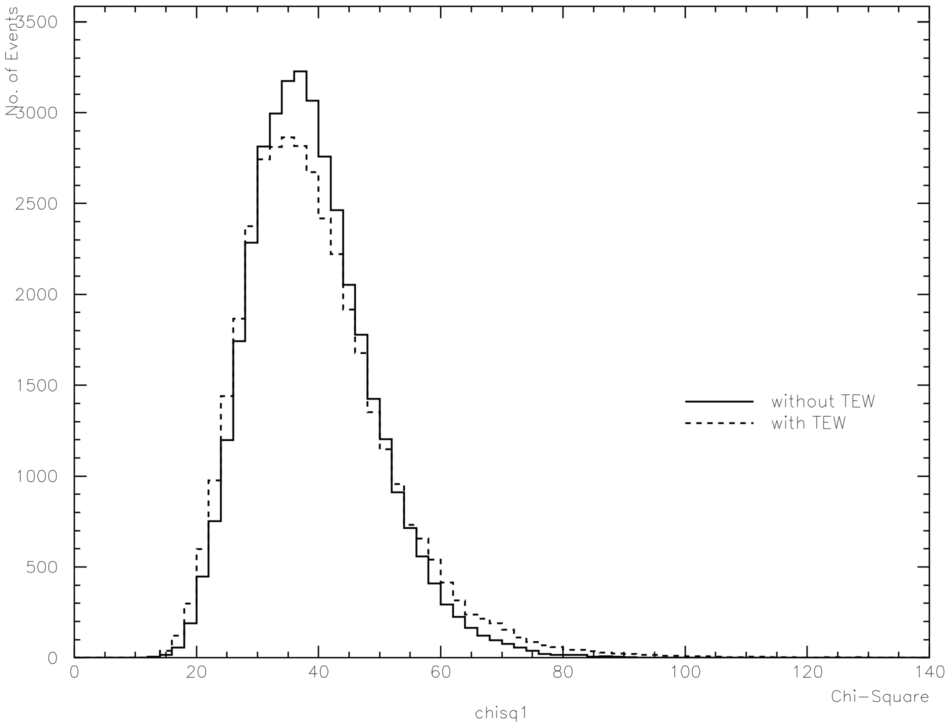

Figure 13: Correlation Chi-Square, Simulated e- with E_{Tot} from 3 to 9 MeV

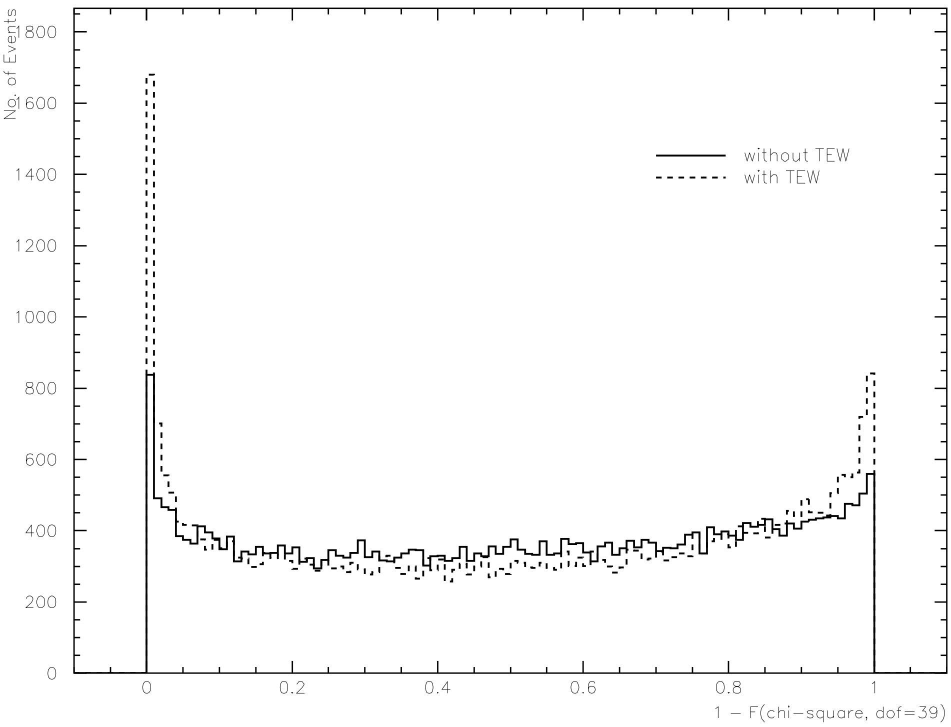

Figure 14: 1 – F(Chi-Square), Simulated e- with E_{Tot} from 3 to 9 MeV

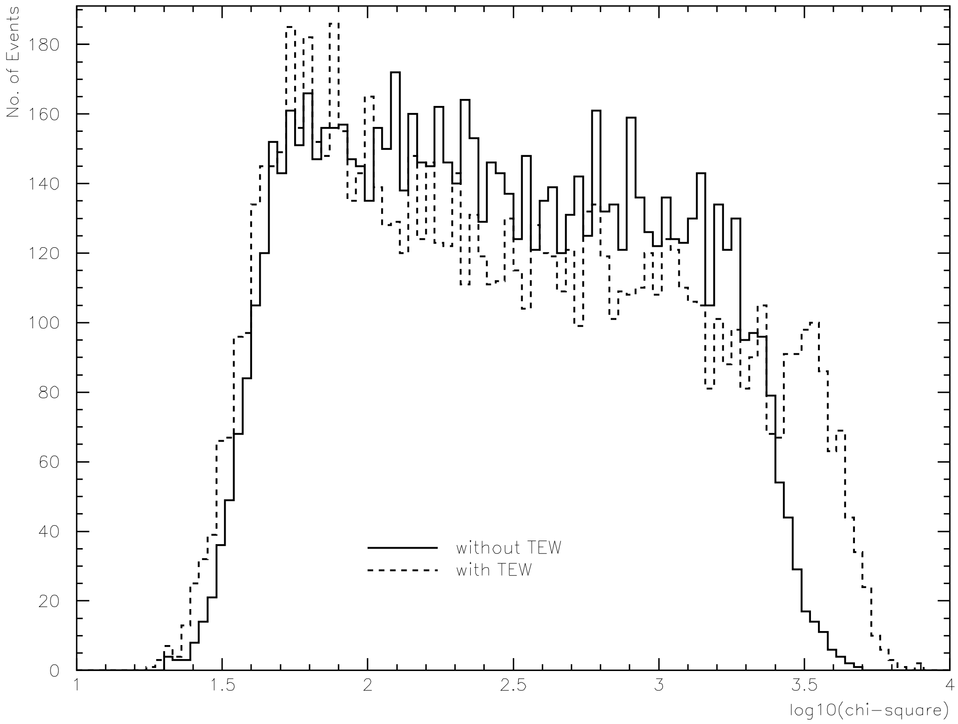

Figure 15: Correlation Chi-Square - Fake Blind Flashers Reconstructed Inside the AV

150. About 14% of the FBFs had N_{hit} values greater than this. For these events, the available standard function with the largest N_{hit} was used to calculate the correlation chi-square.

Figure 15 shows the results on a logarithmic scale. What is of particular interest of course is the degree to which these distributions differ from those of the electron events. To make a comparison, the cumulative distribution functions for all four cases were calculated, normalized to integrate to one over the full range. They are shown in Figure 16. From these graphs, it appears that a cut that removes events above some maximum allowed value should allow one to eliminate about 80% of the fake blind flashers at the cost of a few per cent of the genuine Čerenkov events. Furthermore, a cut based on the correlation chi-square calculated without the TEW should be more efficient because there is a larger separation of the curves for those cases in the range close to the maximum of the electron functions, which is where one would want to place the cut.

Figure 17 is a graph of the fraction of the fake blind flashers cut as a function of the fraction of electron events lost, without and with the TEW. A cut based on the correlation chi-square calculated without application of the time exclusion window is more efficient, resulting in a larger fraction of flashers cut for a given loss of electron events. Based on these results, one can expect to eliminate about 80% of the fake blind flashers that reconstruct inside the AV with a loss of less than 1% of electron-initiated Čerenkov events.

Another statistic besides the correlation chi-square was evaluated for effectiveness in separating fake blind flashers from electron-initiated events. The correlation function for each event was integrated starting at –1 up to varying upper limits, and compared with the corresponding value for the standard correlation function. The greatest absolute difference between the two integrals over the range of upper limits from –1 to +1 was found. (In the following discussion this statistic is referred to as the "maximum delta CCF". It is the same statistic as used in the Kolmogorov-Smirov test.) Figures 18 and 19 show the distributions of the maximum delta CCF for the electron-initiated events and the fake blind flashers. Figure 20 shows the cumulative distribution functions and Figure 21 is the cut efficiency plot. The maximum delta CCF is more efficient when used with the time exclusion window, and with the TEW is more efficient than the correlation chi-square at larger sacrifice values. The maximum delta CCF has the additional advantages of being much easier to calculate, and requiring less data to define a standard case. That is, one needs only the correlation function for the standard case, whereas to calculate the correlation chi-square one must also have calculated the inverse of the covariance matrix. However, the efficiency of the maximum delta CCF appears to be more sensitive to which PMTs are included in its calculation.

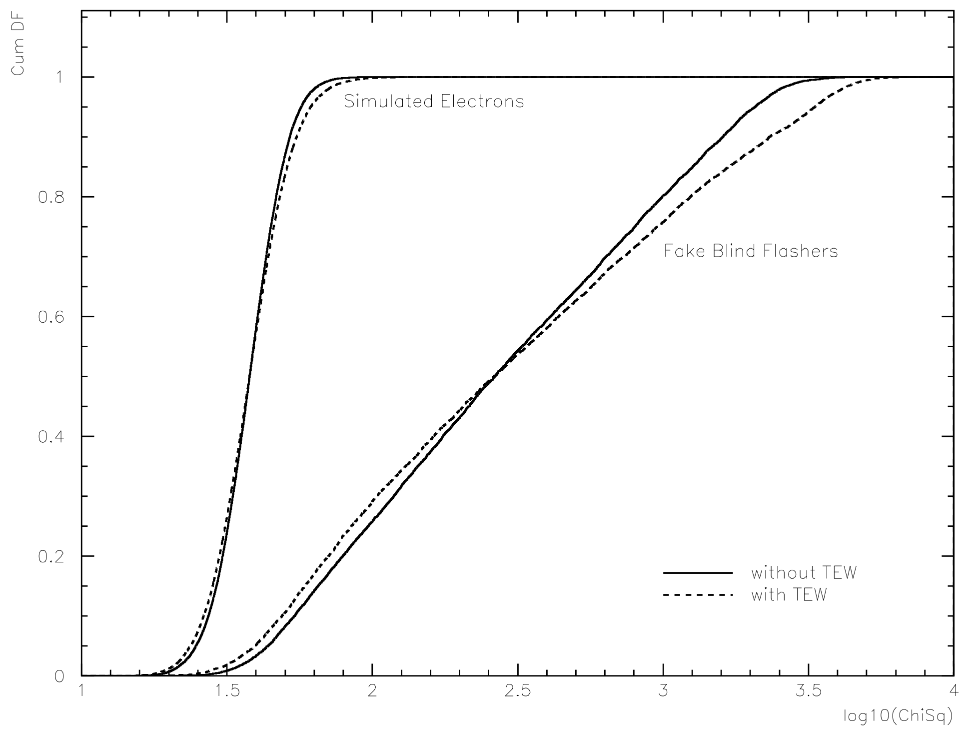

Figure 16: Cumulative Distribution Functions of the Correlation Chi-Squares

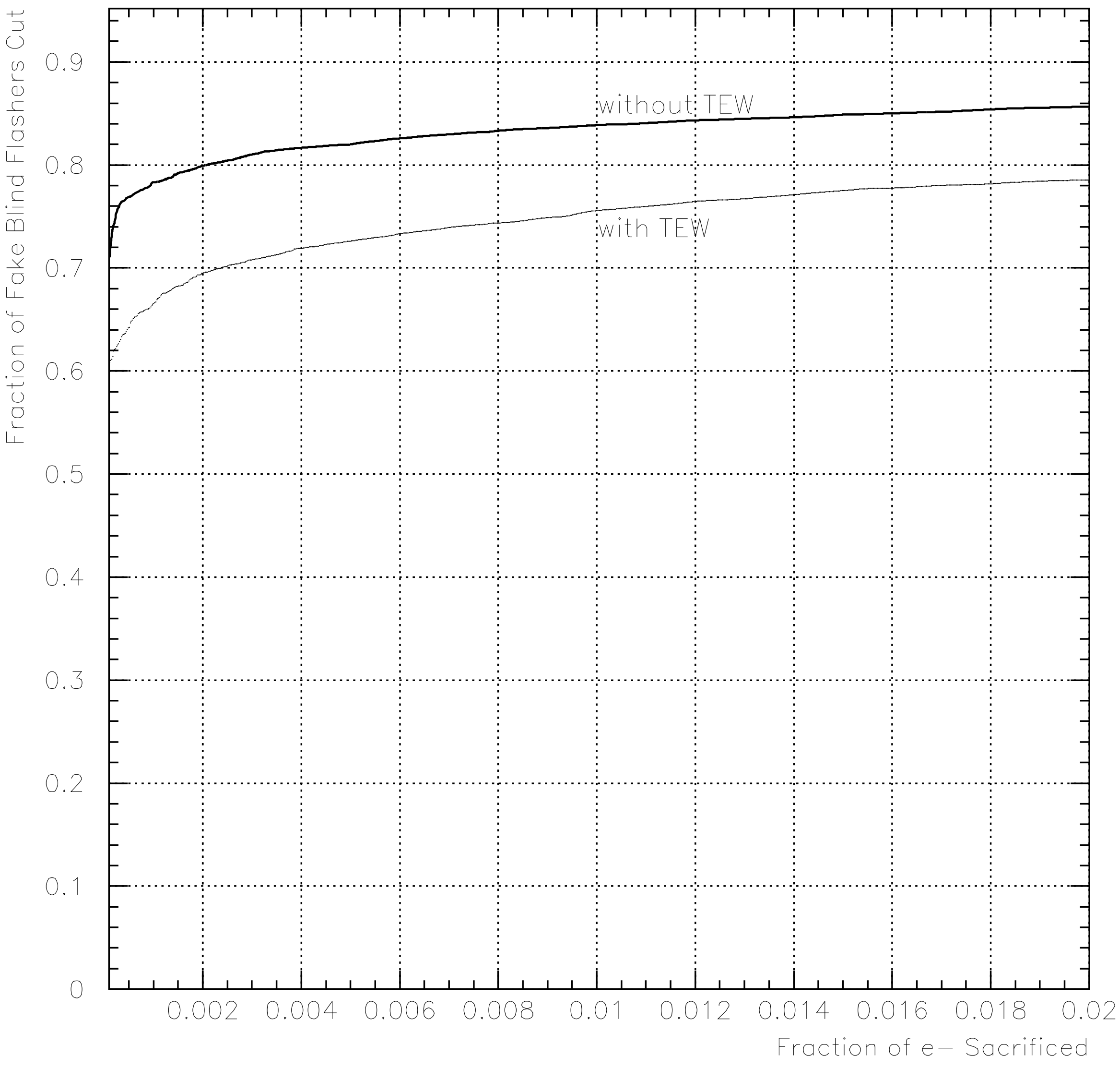

Figure 17: Efficiency of a Cut Based on the Correlation Chi-Square

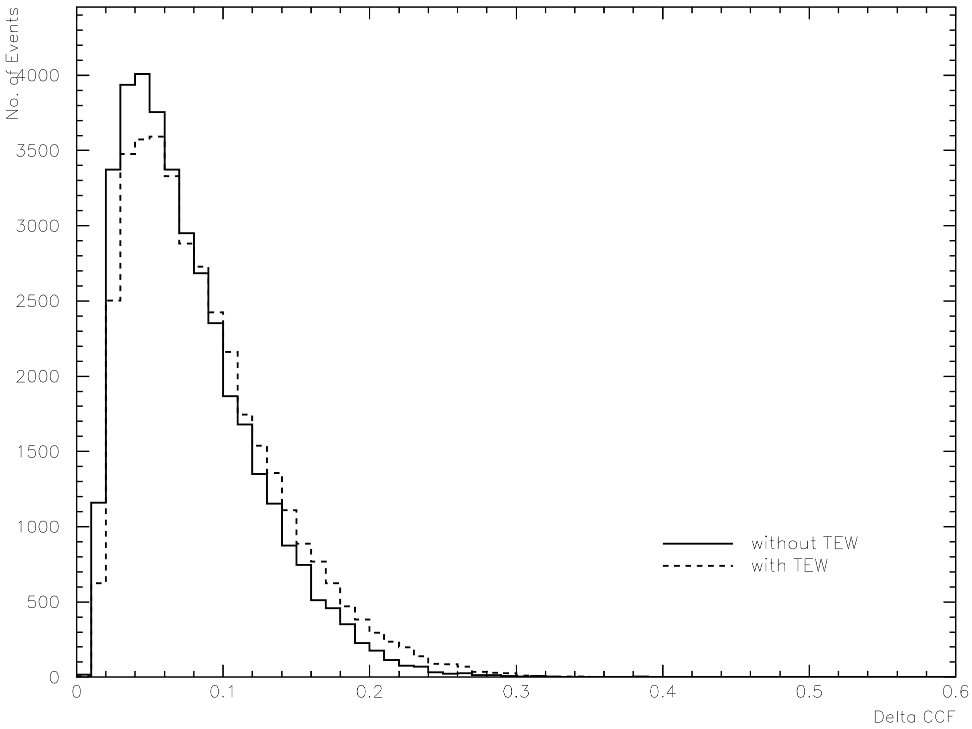

Figure 18: Distribution of Maximum Delta CCF, Electron-Initiated Events

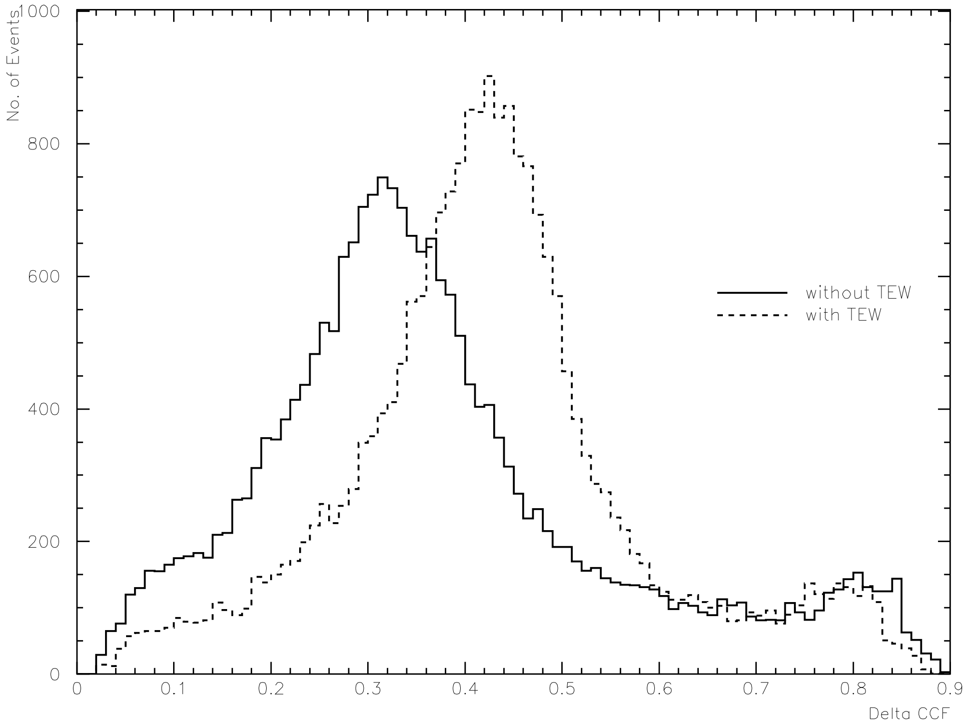

Figure 19: Distribution of Maximum Delta CCF, Fake Blind Flashers

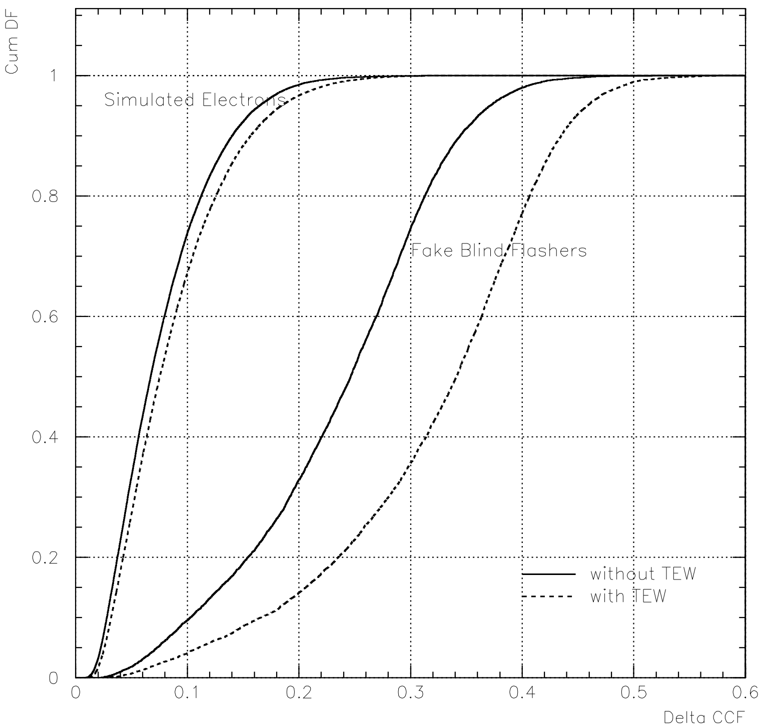

Figure 20: Cumulative Distribution Functions of the Maximum Delta CCF

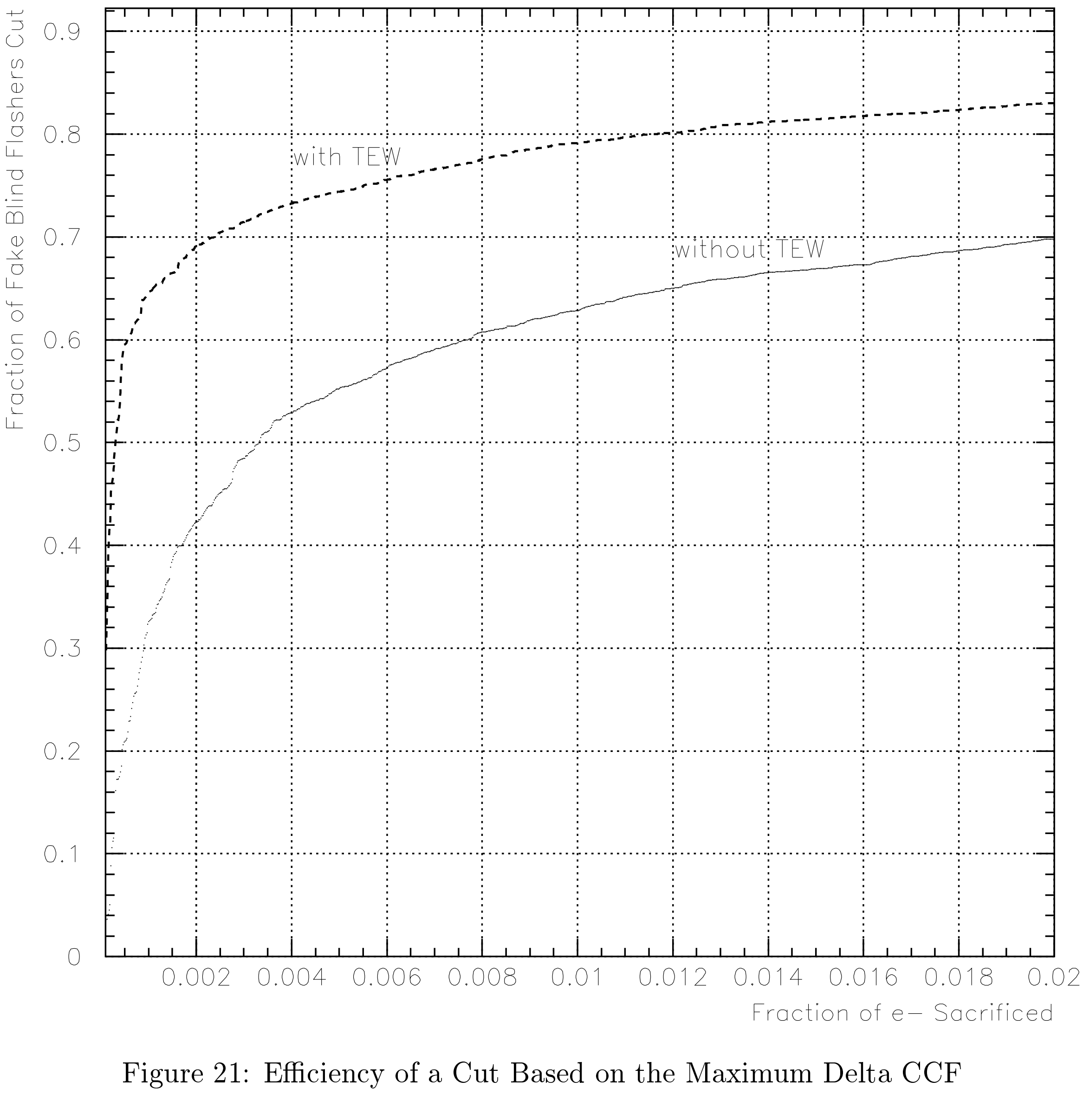

Figure 21: Efficiency of a Cut Based on the Maximum Delta CCF